Biochimica et Biophysica Acta 1840 (2014) 3299–3310

Contents lists available at ScienceDirect

Biochimica et Biophysica Acta

journal homepage: www.elsevier.com/locate/bbagen

A comparison of ceruloplasmin to biological polyanions in promoting the oxidation of Fe^{2+} under physiologically relevant conditions

Bruce X. Wong [a], Scott Ayton [a], Linh Q. Lam [a], Peng Lei [a], Paul A. Adlard [a], Ashley I. Bush [a,*], James A. Duce [a,b,**]

[a] Oxidation Biology Unit, The Florey Institute of Neuroscience and Mental Health, The University of Melbourne, Parkville, Victoria, Australia
[b] School of Molecular and Cellular Biology, Faculty of Biological Sciences, University of Leeds, Leeds, West Yorkshire, United Kingdom

ARTICLE INFO

Article history:
Received 13 June 2014
Received in revised form 31 July 2014
Accepted 14 August 2014
Available online 23 August 2014

Keywords:
Ferroxidase
Ceruloplasmin
Transferrin
Iron
Oxidation

ABSTRACT

Background: Iron oxidation is thought to be predominantly handled enzymatically in the body, to minimize spontaneous combustion with oxygen and to facilitate cellular iron export by loading transferrin. This process may be impaired in disease, and requires more accurate analytical assays to interrogate enzymatic- and auto-oxidation within a physiologically relevant environment.
Method: A new triplex ferroxidase activity assay has been developed that overcomes the previous assay limitations of measuring iron oxidation at a physiologically relevant pH and salinity.
Results: Revised enzymatic kinetics for ceruloplasmin ($V_{max} \approx 35$ μM Fe^{3+}/min/μM; $K_m \approx 15$ μM) are provided under physiological conditions, and inhibition by sodium azide (K_i for Ferric Gain 78.3 μM, K_i for transferrin loading 8.1×10^4 μM) is quantified. We also used this assay to characterize the non-enzymatic oxidation of iron that proceeded linearly under physiological conditions.
Conclusions and general significance: These findings indicate that the requirement of an enzyme to oxidize iron may only be necessary under conditions of adverse pH or anionic strength, for example from hypoxia. In a normal physiological environment, Fe^{3+} incorporation into transferrin would be sufficiently enabled by the biological polyanions that are prevalent within extracellular fluids.

1. Introduction

Iron is an essential element for most forms of life, however iron overload can be toxic. The ability for iron to undergo redox cycling in physiological conditions underlies both its biochemical utility, and its potential hazard. Iron transitions in active sites from and to ferric (Fe^{3+}) and ferrous (Fe^{2+}) forms [1,2] to catalyze enzymatic processes. However, this versatility can also have potentially detrimental effects where free Fe^{2+} and Fe^{3+} ions partake in Haber–Weiss [3] and Fenton [4] redox reactions to generate chemically reactive hydroxyl radicals and superoxide that degrade lipids, proteins and nucleic acids [5–7]. Therefore, to prevent iron-induced toxicity, organisms that are iron-dependent have protein chaperones and transporters to maintain iron homeostasis, trafficking and metabolism [8].

Ferroxidases are considered to play an important role in the efflux of iron from cells. It is thought that exiting iron is in the ferrous state when transported across the plasma membrane through the transmembrane pore ferroportin (FPN). Upon reaching the extracellular surface, iron must be oxidized to its Fe^{3+} state before being released from FPN and being incorporated into the extracellular transport protein, transferrin (TF). Traditionally multicopper ferroxidases such as ceruloplasmin (CP) and hephaestin are considered to not only stabilize FPN on the cell surface [9,10] but also utilize copper to oxidize iron and facilitate efflux [11–13]. Evidence supporting this role for multicopper ferroxidases was shown when perfused livers of copper-deficient dogs and pigs that had accumulated iron were treated with holo-CP resulting in immediate release of iron into the periphery [14–16]. Humans [17] and rodents [18] affected by aceruloplasminemia (absence of CP) accumulate iron, but only slowly, indicating that iron export from tissue is handled by mechanisms that might have some redundancy. One possible explanation is that under conditions of adequate oxygenation, biological polyanions such as citrate and phosphate can sufficiently promote ferroxidation by altering the Fe^{2+}/Fe^{3+} redox couple, without the need for a ferroxidase [19]. Mammalian blood [20] and CSF [21] have been reported to contain low molecular weight ferroxidation activities that might reflect this chemistry [20,21]. This underscores a proposal that ferroxidase enzymes like CP might only be needed under conditions of hypoxic stress, where their low K_m for O_2 enables them to promote ferroxidation where a polyanion cannot [19].

Consistent with the possibility that CP is mainly active under hypoxic conditions, loss of CP activity has been reported in serum [22–27],

* Corresponding author.
** Correspondence to: J.A. Duce, School of Molecular and Cellular Biology, Faculty of Biological Sciences, University of Leeds, Leeds, North Yorkshire, United Kingdom.
E-mail addresses: ashleyib@unimelb.edu.au (A.I. Bush), J.A.Duce@leeds.ac.uk (J.A. Duce).

http://dx.doi.org/10.1016/j.bbagen.2014.08.006

cerebrospinal fluid (CSF) [28–30], and brain [31–33] in Alzheimer's disease (AD) and Parkinson's disease (PD) conditions where oxidative stress and hypoxia have been implicated. The inability of CP to be recruited for the export of iron under hypoxic conditions may explain the toxic accumulation of iron in the brain in these diseases [34–37].

While these findings argue that the study of ferroxidases in neurodegenerative disease warrants further attention, the tools for their study are problematic. Ferroxidase activity is frequently measured by the colorimetric assay developed by Osaki, Johnson and Frieden [2,38] that requires Fe^{2+} and apo-TF as substrates and monitors spectroscopic change to TF upon incorporation of Fe^{3+}. Originally used to measure 'ferroxidase I' enzyme activity in serum, that was later determined to be CP, this method has since been used to define the ferroxidase activity of H-ferritin [39], hephaestin [40] and β-amyloid precursor protein [33]. Later colorimetric methods for measuring the oxidation of iron have made use of Fe^{2+}-specific chromogens such as ferrozine [40,41] and ferene *S* [20,42]. Also, direct measurement of Fe^{3+} spectrophotometrically has been performed to monitor the activity of ferroxidases [20,43,44]. Each of these assays has their own limitations and caveats. The "transferrin assay" [38] is an indirect measure of ferroxidase activity that could be restricted by the loading rate of Fe^{3+} onto apo-TF instead of actual catalytic oxidation activity. This is further complicated by TF also accelerating the rate of reaction and possibly having oxidase activity itself [45]. The "Ferrous Loss assay" [20,42] also indirectly measures ferroxidase activity through selective chelation of the remaining Fe^{2+} with a chromagen, e.g. ferene *S*. It cannot be used for kinetic measurements because it competes with the enzyme for Fe^{2+}, thus inhibiting ferroxidation if present at the beginning of the assay. The "Ferric Gain assay" [20,43,44] is the only direct measurement of ferroxidase activity but uses an absorbance wavelength of 310 nm to monitor Fe^{3+}, which overlaps with the absorbance spectra of many proteins. Most significantly, the buffer used in the development of each of these assays was pH ≈ 6 sodium acetate (NaOAc), to minimize auto-oxidation. Not only is NaOAc outside of its buffering range at pH 6, but saline was also not adjusted to isotonic levels [2,20,38,39,42] rendering these classical assay systems unsuitable for assessing iron oxidation under physiological conditions.

In the current study, effort has been taken to design a method to measure ferroxidase activity in a manner that combines the advantages of each of these existing assays while utilizing our better present understanding of iron oxidation to remedy the disadvantages of the previously used parameters. The combined kinetic assay provides a more comprehensive representation of the ferroxidase activity within a physiological environment and has enabled the characterization of the ferroxidase activity of CP under physiologically relevant conditions, as well as the inhibitory effects of sodium azide on its catalytic ferroxidase activity.

2. Experimental procedures

2.1. Reagents

Reagents were all of analytical grade and were purchased from Sigma, Australia, unless otherwise stated.

2.2. Reagent preparations

Purity of human CP (Vital Products) and bovine serum albumin (BSA) was enhanced by size exclusion with a Superdex 200 10/GL filtration column (GE Healthcare) and buffer-exchanged into either HBS (HEPES 50 mM, NaCl 150 mM, pH 7.2) or double-distilled water (ddH_2O) by repeated washes through a 30 kDa cutoff Amicon Ultra-15 (Millipore) centrifugal filter unit, or by dialysis (Thermo Scientific) with a 10 kDa cutoff membrane. Subsequent flow-through or dialysis buffer was used as the vehicle controls for the ferroxidase assay. The buffer-exchanged proteins as well as human apo-transferrin (>98% pure) dissolved in ddH_2O were quantified through bicinchoninic acid (BCA) assay (Pierce) according to the manufacturer's protocol.

Ferrous ammonium sulfate or ferrous sulfate solution was prepared by dissolving a known amount in N_2-flushed ddH_2O immediately prior to the commencement of experiments. The ferrous sulfate substrate was used within a one hour period when auto-oxidation was still observed as negligible (illustrated as 'vehicle control' in all figures).

2.3. Ferroxidase assays

A ferroxidase is an enzyme that catalyzes the oxidation of Fe^{2+} to Fe^{3+} with the liberation of water from oxygen. Three previously established procedures were adapted in a plate assay to spectrophotometrically measure substrate (Fe^{2+}) or products (Fe^{3+} and diferric holo-TF) involved in the ferroxidase reaction.

2.4. 'Ferrous Loss' assay

Adapted from Erel et al. [42], the first procedure measured Fe^{2+} consumption by loss of absorbance at 590 nm from selective Fe^{2+} binding to the chromogen ferene *S*. (Eqs. (1) and (2)):

$$Fe^{2+} \overset{Cp\ e^-}{\rightleftharpoons} Fe^{3+} \tag{1}$$

$$Fe^{2+} + \text{ferene } S \rightleftharpoons Fe^{3+} : \text{ferene } S\ (Abs_{590nm}). \tag{2}$$

2.5. 'Ferric Gain' assay

The second procedure from Minotti and Ikeda-Saito [44] directly measured Fe^{3+} conversion by change in 310 nm absorbance (Eq. (3)).

$$Fe^{2+} \overset{Cp\ e^-}{\rightleftharpoons} Fe^{3+}\ (Abs_{310nm}) \tag{3}$$

2.6. TF loading assay

A third procedure adapted from Johnson et al. [2] as well as Bakker and Boyer [39] followed the physiological loading of apo-TF with Fe^{3+} which resulted in a change of absorbance at 460 nm (Eq. (4) or (5)).

$$\underset{K_m}{Fe^{2+} \overset{Cp\ e^-}{\rightleftharpoons} Fe^{3+}} \underset{K_a}{+ Tf \rightleftharpoons Tf : Fe^{3+}}\ (Abs_{460nm}) \tag{4}$$

or

$$\underset{K_a}{Fe^{2+} + Tf \rightleftharpoons Tf : Fe^{2+}} \underset{K_m}{\overset{Cp\ e^-}{\rightleftharpoons} Tf : Fe^{3+}}\ (Abs_{460nm}) \tag{5}$$

In 200 μL reaction mixes (final concentrations): enzyme (500 or 250 nM) was added to HBS (HEPES 50 mM, NaCl 150 mM, pH 7.2) (unless otherwise stated) in the absence or presence of apo-TF (50 μM). Either ferrous ammonium sulfate or ferrous sulfate (100 μM) was able to be used as substrates for the assay and was dissolved in N_2-purged ddH_2O just prior to addition. The substrate was added as the last component of the assay to initiate the reaction. Absorbance readings (310 nM and 460 nM) were monitored at 30 s intervals over 4 min at 24 °C with agitation. Ferene *S* (500 μM) was added at

the end of 4 min, briefly agitated and absorbance (590 nm) was read immediately. For experiments involving enzyme rates the reactions were monitored for 3 min when the ferroxidase reaction was still linear. Refer to Figure S1 for the workflow of preparation of triplex assay. Reactions were blanked against sample buffers (HBS) that had all components in the reaction mix except the sample itself. Extinction coefficients of Fe were recalculated for the new assay as shown in Table 1 on either the Flexstation 3 (Molecular Devices) or PowerWave HT (BioTek) microplate spectrophotometer. Results were plotted and statistically analyzed using a combination of Excel (2011, Microsoft) and Prism (v5.0. GraphPad Software Inc.).

3. Results

We began the development of a multiple ferroxidase assay by examining the impact of various buffer conditions upon the TF loading assay, with the aim to identify suitable solutions that could be applied to the assay of candidate ferroxidase enzymes under physiological conditions of pH and saline.

3.1. Adaptation of the transferrin loading assay

Spectral changes occurring during the TF loading reaction are illustrated in Fig. 1Ai–ii. After 10 min, only in the combined presence of CP, TF and Fe^{2+} there is an increase in absorbance at 460 nm with all other component controls giving negligible measurements at the same wavelength.

Further assay development required only one component of the TF loading assay to be investigated while all the other components were kept constant according to the methods by Johnson et al. [2] and Bakker and Boyer [39]. Increasing CP, apo-TF or Fe^{2+} resulted in increased rate of Fe^{3+} formation, while increasing NaOAc buffer concentrations decreased CP activity (Fig. 1B–E). These results indicate that, despite the NaOAc buffer being outside its buffering range (pH 3.6–5.6) [46], the conditions used previously [2,39] were still suitable for the TF loading assay at pH 6, namely 100 mM NaOAc buffer, 250 nM CP; 50 μM apo-TF; and 100 μM ferrous ammonium sulfate or ferrous sulfate.

As the non-buffered environment currently used in the assay may result in anomalous outcomes caused by iron auto-oxidation [47] alternative buffers within their buffering range were tested. The buffers, including Good's buffers, were grouped into low pH (pH 5.5–6.0), neutral pH (pH 7.0) and physiological (isotonic saline, pH 7.4) (Fig. 2A–C). At low pH, NaOAc buffer at pH 5.5 provided the best performance in the TF loading assay, while at neutral pH HEPES and PIPES were the best candidates. In physiological conditions HEPES-buffered saline (HBS) was best for measuring TF loading. CP activity in loading TF was abolished by citrate buffer (Fig. 2B), potentially due to citrate sequestering available iron from TF [45]. Interestingly, phosphate-buffered saline (PBS) increased the overall rate of TF loading compared to other buffer systems (Figs. 2C and S2), possibly because the phosphates present within this buffer promote auto-oxidation by interacting with Fe^{3+} ions and transferring them to TF [48].

Having identified the best working buffers within the experimental conditions required for TF loading with minimal auto-oxidation, the best pH within each buffering range was shown to be 5.5 for NaOAc, 6.5 for PIPES and 7.0 for HBS (Fig. 3A–C). To accurately measure ferroxidase activity, enzymatic rate should be much greater than the rate of auto-oxidation of Fe^{2+}. CP had little to no ferroxidase activity when pH was ≤5.0, but from pH 5.5 to 7.5, activity increased linearly at 0.011 ± 0.001 AU/min/pH ($r^2 = 0.951$) with a V_{max} of 0.029 ± 0.001 AU/min (Fig. 3Di). However, the rate of iron auto-oxidation increased markedly above pH 7.0 and reached a rate comparable to CP enzymatic activity at pH 8.0 (Fig. 3Di). Blanking the activity of CP against the vehicle control highlighted the influence of pH on TF loading activity and underscored the contribution of Fe^{2+} auto-oxidation to TF loading at physiological pH. The usable pH range for TF loading assay was 5.5–7.5, optimally pH 7.2 to discern the contribution of CP above such auto-oxidation (Fig. 3Dii).

The effect of salinity was investigated by NaCl titration in 50 mM HEPES buffer pH 7.2, representing physiological pH. Increasing salinity from 0–200 mM had minimal effect on the TF loading ferroxidase activity of CP, but induced a concentration-dependent suppression of Fe^{2+} auto-oxidation (Fig. 4i–ii). Upon blanking CP against vehicle auto-oxidation it was apparent that increasing salinity did not alter the rate of CP activity but lengthened the time before Fe^{2+} auto-oxidation was comparable to CP activity; as illustrated when activity reached a plateau (Fig. 4iii). This lengthening of time effectively allows a greater window for data collection on CP activity. As a salinity of 150 mM is physiological yet suppresses auto-oxidation, this concentration was chosen for further experimental conditions.

In summary, the TF loading assay performed adequately in NaOAc (100 mM, pH 5.5), PIPES (100 mM, pH 6.5) or HBS (50 mM HEPES, 150 mM NaCl, pH 7.2) (Fig. 5Ai–iii), with components of 50 μM apo-TF, 250 nM CP and 100 μM ferrous sulfate. Within these conditions, temperature was kept at 24 °C and rate measurements of CP activity were taken within the first 3 min when the rate is in its linear phase (Fig. 5Bi–iii. respectively).

3.2. Determining iron extinction coefficients in all three ferroxidase assays using optimal parameters for transferrin loading

The same conditions derived for the "TF loading" ferroxidase assay at pH 5.5 (NaOAc), 6.5 (PIPES) and 7.2 (HBS) were applied to the two other ferroxidase assays that measure ferrous loss and ferric gain. CP-catalyzed ferroxidation was found to be clearly greater than Fe^{2+} autoxidation in all three assays using these conditions (data not shown). To validate the reproducibility of results in different spectrophotometric instruments, the Ferrous Loss assay was studied by titration of Fe^{2+}. No difference in linear gradient absorbance was observed between instruments when pathlength-correction was applied (data not shown). In addition, total volume size after pathlength-correction did not affect the outcome (data not shown). Therefore, this assay is obust between instruments as long as absorbance readings are corrected for pathlength.

The extinction coefficient of ferrous loss was experimentally derived through a standard curve of Fe^{2+}–ferene *S* complex in NaOAc, PIPES or HBS buffers following the Beer–Lambert law. A standard curve of Fe^{2+} concentration (0–200 μM) was derived at a fixed molar excess of ferene *S* (500 μM). It was noted that varying the concentrations of ferene *S* at a constant iron concentration altered the absorbance readout (data not shown). The assumptions for calculating the extinction coefficient in this assay were; accuracy of stock $FeSO_4$ concentration and that all Fe^{2+} had complexed with ferene *S* or was in equilibrium before each measurement was taken. The standard curve proceeded linearly until

Table 1
Experimentally-derived extinction coefficients for new ferroxidase assay.

	Ferrous loss (mM^{-1} Fe^{2+} cm^{-1})	Ferric gain (mM^{-1} Fe^{3+} cm^{-1})	Transferrin loading (mM^{-1} Fe^{3+} cm^{-1})
Sodium acetate buffer, pH = 5.5	37.3	2.30	0.756
PIPES buffer, pH = 6.5	37.3	1.93	2.28
HBS, pH = 7.2	36.6	2.01	2.02

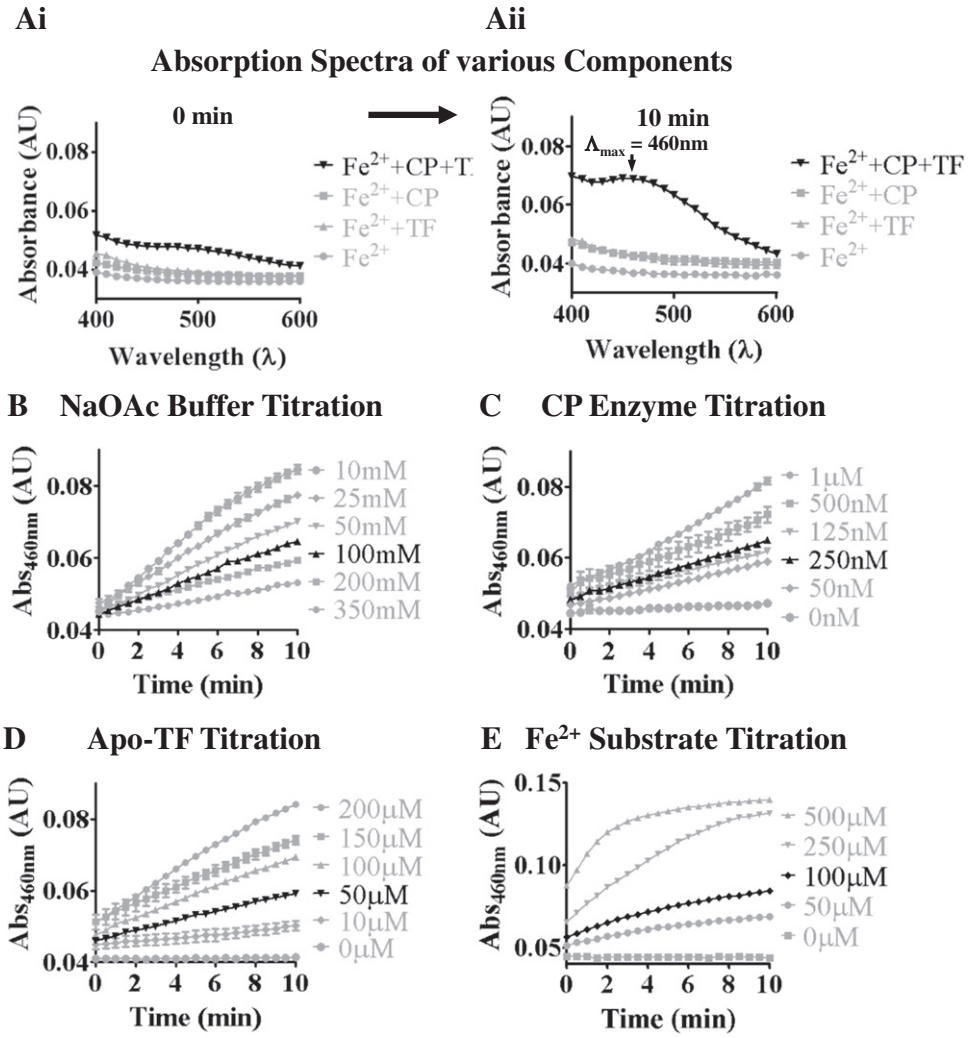

Fig. 1. Optimisation of the transferrin loading assay conducted in sodium acetate buffer pH 6. (A) Absorbance spectra of Fe^{2+} in the absence or presence of assay components at time point 0 (i) and 10 min (ii). Kinetic assay depicting the changes in absorbance at 460 nm when sodium acetate (NaOAc; pH 6) (B), CP (C) apo-transferrin (TF) (D) and ammonium ferrous sulfate (E) are titrated into the assay while the other components are set to the concentrations originally used by Johnson et al. [2]. Results for the ferrous sulfate substrate were identical to ammonium ferrous sulfate (data not shown). For the TF loading assay in NaOAc pH 6, results in black were selected as the recommended conditions; NaOAc buffer (100 mM), apo-TF (50 μM), CP (250 nM) and ammonium ferrous sulfate (100 μM). Assays were run at 37 °C and all results with CP present were blanked against appropriate vehicle controls. Individual data points were mean ± standard error (S.E.) ΔAbs_{460} of 2 experiments done in duplicates.

100 μM $FeSO_4$ (ε = 37.3 mM^{-1} Fe^{2+} cm^{-1} in NaOAc and PIPES; ε = 36.6 mM^{-1} Fe^{2+} cm^{-1} in HBS, r^2 = 0.999 for all), after which a plateau was reached due to the ceiling value of the instrument (Table 1).

Deriving the extinction coefficient of the Ferric Gain assay was carried out in an independent assay using the same titration concentrations of $FeSO_4$ as above. For this assay complete oxidation by CP was required in the various buffers. To ensure this, absorbance was measured at 310 nm up to 96 h. All endpoint measurements indicated that the oxidation reaction had gone to completion by 24 h. The standard curve proceeded linearly for NaOAc (average ε = 2.30 mM^{-1} Fe^{2+} cm^{-1}, r^2 = 0.879); PIPES (average ε = 1.93 mM^{-1} Fe^{2+} cm^{-1}, r^2 = 0.968); and HBS (average ε = 2.01 mM^{-1} Fe^{2+} cm^{-1}, r^2 = 0.846) (Table 1). In NaOAc a titration of $FeSO_4$ without CP did not reach the levels of oxidized Fe^{3+} obtained with CP even by 96 h, but in the presence of PIPES or HBS similar levels of Fe^{3+} were obtained by auto-oxidation at intervals longer than 48 h (data not shown).

Similar to the Ferric Gain assay, the extinction coefficients for the TF loading assay in the various buffers were derived from a titration of $FeSO_4$ in the presence of TF (50 μM) ± CP. The standard curve proceeded linearly for NaOAc (average ε = 0.756 mM^{-1} Fe^{2+} cm^{-1}, r^2 = 0.808); PIPES (average ε = 2.28 mM^{-1} Fe^{2+} cm^{-1}, r^2 = 0.969); and HBS (average ε = 2.02 mM^{-1} Fe^{2+} cm^{-1}, r^2 = 0.971) (Table 1). As with the Ferric Gain assay, auto-oxidation of Fe^{2+} in the TF loading assay was markedly delayed but did eventually reach the same levels as in the presence of CP (data not shown).

3.3. Characterizing ferroxidase activity using the new combined assay

The ferroxidase activity of CP was determined in a single plate spectrophotometric assay +/− TF to examine the rate of ferrous loss, ferric gain and apo-TF loading in parallel using HBS (pH 7.2) buffer to represent more physiologically relevant conditions than the canonical characterization [2,20,38,39,42]. The rate of CP ferroxidase activity without apo-TF was 11.72 ± 0.48 μM Fe^{3+}/min (r^2 = 0.984) for 250 nM CP (Fig. 6A), however this rate for CP was greatly enhanced by the presence of apo-TF (28.96 ± 0.96 μM Fe^{3+}/min, r^2 = 0.989). Apo-TF alone facilitated iron oxidation (2.85 ± 0.24 μM Fe^{3+}/min, r2 = 0.934) (Fig. 6B), compared to vehicle alone (0.348 ± 0.08 μM Fe^{3+}/min, r2 = 0.673) as previously reported [45,49]. Upon correcting for oxidation in the presence of apo-TF only, the rate of CP ferroxidase activity in the presence of TF was still more than twice the rate of CP ferroxidase without TF (26.10 ± 1.00 μM Fe^{3+}/min). This indicated that there is cooperation between CP and TF. The addition of

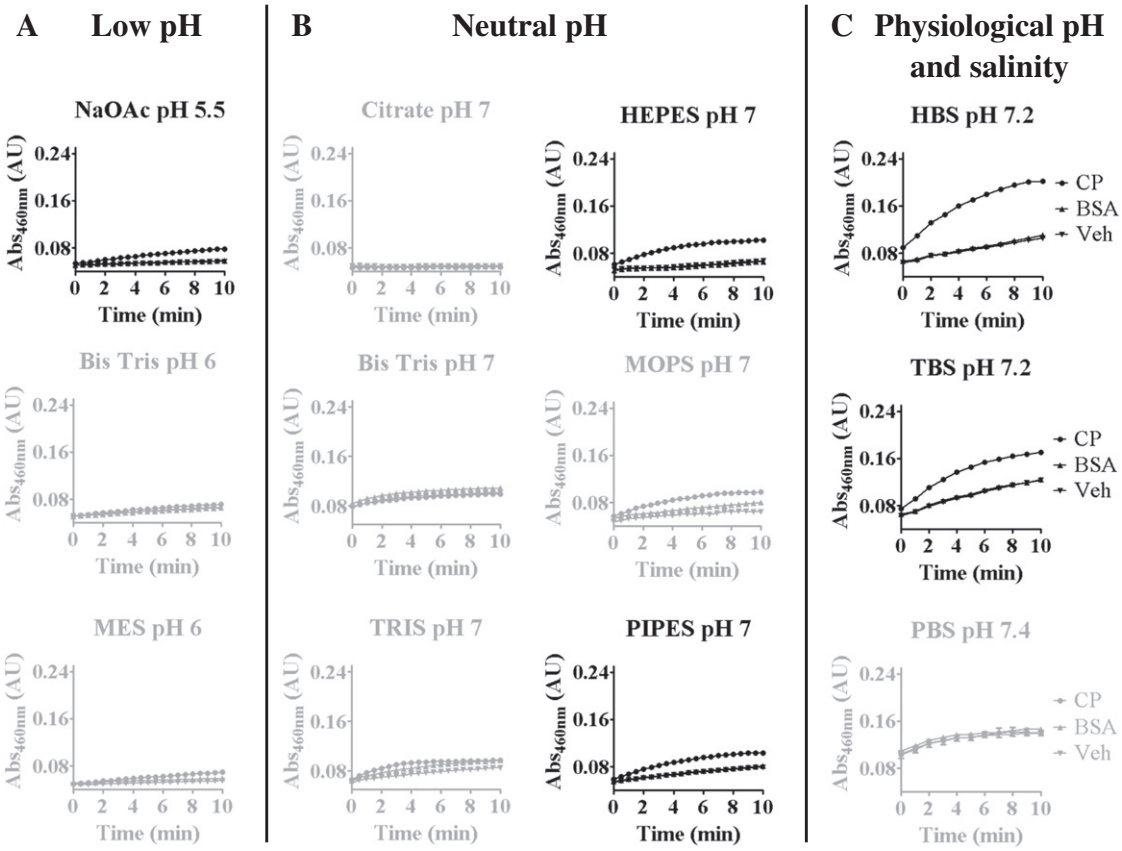

Fig. 2. Buffer effects on transferrin loading assay. Buffers were grouped according to pH and salinity with low pH (100 mM buffer) ranging from pH 5.5–6 and no NaCl (A), neutral pH (100 mM buffer) at pH 7.0 and no NaCl (B), and physiological pH (50 mM buffer) at pH 7.2–7.4 with 150 mM NaCl (C). Results in black indicate suitable buffers for the transferrin loading assay with all other components required for the assay fixed at the final concentrations determined in Fig. 1, but the assay was performed at 24 °C to slow the rate of oxidation. Individual data points were means ± S.E. ΔAbs_{460} of 1 experiment done in triplicates.

ferene *S* to determine ferrous loss at the end of the 3 min linear phase served to confirm results observed in the Ferric Gain and TF loading assays. After 3 min 35.2 μM Fe^{3+} was detected by the Ferric Gain assay compared to 44.1 μM Fe^{3+} in the Ferrous Loss assay (Fig. 6A & C). This ~10 μM Fe^{3+} discrepancy may have been caused by the delay taking the plate out of the spectrophotometer and manually adding the ferene *S* chromogen. Fe^{3+} between TF loading and Ferrous Loss assays was more comparable (86.9 μM Fe^{3+} and 87.1 μM Fe^{3+} respectively) (Fig. 6B & D). Taken together, these results confirm that the combined ferroxidase assay is robust, quantitative and comparable between individual assays.

3.4. Enzyme kinetic characterization of ceruloplasmin

Utilizing the new combined assay in a physiologically appropriate buffer (i.e. HBS pH 7.2), Michaelis–Menten enzyme kinetics of CP ferroxidase activity was calculated. As expected for an enzymatic reaction, the velocity of CP followed a non-linear regression curve for Ferric Gain and TF loading whereas auto-oxidation proceeded linearly (Fig. 7A & B). In the TF assay, the linear progression of auto-oxidation eventually intersected the regression curve of CP catalyzed oxidation at ~400 μM Fe^{2+} (Fig. 7B). When CP activity was blanked against the appropriate controls, including auto-oxidation, the rate measurements yielded similar K_m values for Ferric Gain and TF loading, but V_{max} values that were slightly different (Ferric Gain: $V_{max} = 38.96 \pm 1.33$ μM Fe^{3+}/min/μM CP; $K_m = 15.07 \pm 2.07$ μM vs. TF loading: $V_{max} = 33.83 \pm 2.06$ μM Fe^{3+}/min/μM CP; $K_m = 15.68 \pm 3.73$ μM) (Fig. 7C, D). A caveat in the accuracy of enzyme kinetics from the TF loading assay is that the readout may have been distorted by transferrin either detecting continual competition for Fe^{2+} by auto-oxidation or facilitating oxidation.

Within our experimental parameters, we also investigated the effects TF may have on CP. By TF loading assay, TF alone promoted Fe^{2+} oxidation at pH 7.2 (Fig. 7A & B). However, because the velocity of this activity proceeded linearly in a substrate-dependent manner, the velocity was more akin to a depletion of substrate (Fe^{2+}) and subsequent shift of equilibrium to increased consumption of products rather than catalysis by an enzyme.

3.5. Inhibition of ceruloplasmin by azide

Azide has previously been reported to inhibit CP amine oxidase activity in vitro [50] and the fraction of the ferroxidase activity represented by CP in serum/plasma [51]. However, as far as we are aware, the inhibition by azide on the ferroxidase activity of CP in vitro has yet to be evaluated. Using the combined ferroxidase assay in HBS (pH 7.2), at a fixed substrate concentration of Fe^{2+} (50 μM), azide was shown to efficiently inhibit CP (250 nM) ferroxidase activity with an IC50 of azide at ~40 μM for Ferric Gain and ~50 μM for the TF loading (Fig. 8A & B).

Previous work on azide inhibition of the amine oxidase activity of CP has indicated uncompetitive inhibition whereby azide directly inhibits the enzyme-substrate complex or forms a complex with CP that incapacitates its activity [50]. Using Lineweaver Burk plots with increasing inhibitor concentrations, we similarly model uncompetitive inhibition by azide in both Ferric Gain and TF loading assays (Fig. 8C & D). The inhibitory constant (αK_i) (inhibitor to enzyme binding) was derived from the product of the binding constant of azide to CP (K_i) and Fe^{2+} to CP (α) as these are unable to be accurately fitted separately for

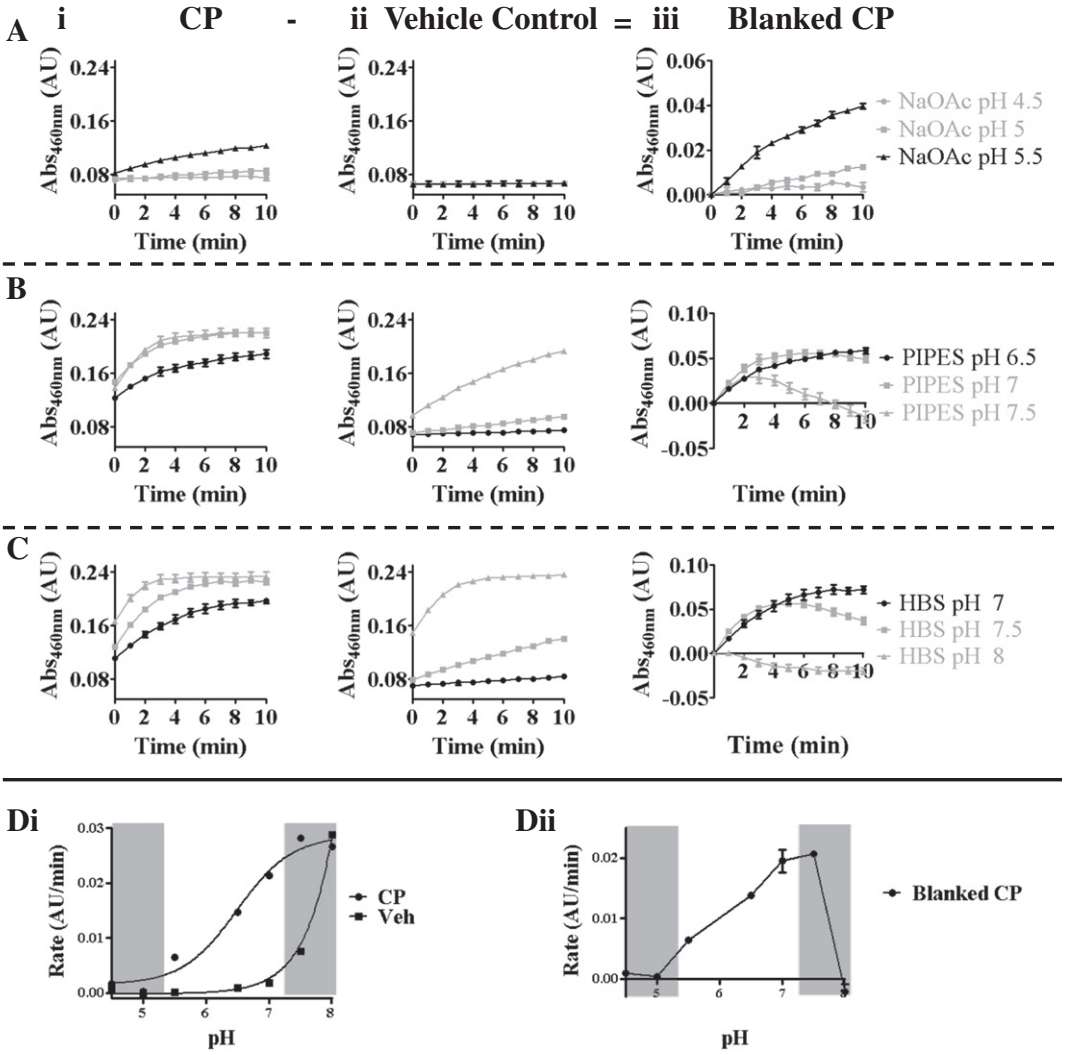

Fig. 3. pH effects in optimal buffers for transferrin loading assay. pH variance on the TF loading assay was investigated in the suggested buffers with low, neutral and physiological pH range (see Fig. 2). NaOAc (100 mM) at pH 4.5–5.5 (A), PIPES (100 mM) at pH 6.5–7.5 (B) and HBS (50 mM HEPES, 150 mM NaCl) at pH 7.0–8.0 (C) were assayed in the presence of CP (250 nM) (i), the corresponding vehicle control (ii) and with CP blanked against the vehicle control (iii). The results in black indicate the recommended pH for each buffer with the final concentrations of the other assay reagents kept constant and the assay ran at 24 °C. The rate of CP activity was plotted at pH 4.5–8.0 (NaOAc, pH 4.5–5.5; PIPES, pH 6.5–7.0; and HBS, pH 7.0–8.0) before (Di) and after (Dii) subtraction of auto-oxidation (shown as vehicle control, Veh, in Di). Experiments were conducted twice with individual data points of the graphs representing means ± S.E. ΔAbs_{460} shown is of 1 representative experiment of 3, with data points as the mean of triplicate readings.

uncompetitive inhibitors [52]. As these double-reciprocal plots do not obey the assumptions of linear regression (due to distortion of experimental error), V_{max}, K_m and αK_i were calculated using non-linear regression (Fig. 8E & F Table 2). Azide as an uncompetitive inhibitor did not bind to the enzyme CP as signified by the high K_i (Ferric Gain was 78.3 ± 47.8 μM and K_i for TF loading was $8.1 \times 10^4 \pm 7.5 \times 10^4$ μM), while α was low indicating that azide enhanced substrate Fe^{2+} binding to enzyme CP (Ferric Gain: 0.39 ± 0.26 and TF loading: 4.1×10^{-4} ±0.38). The model that best fits these results thus confirms the uncompetitive inhibition of azide on CP that was illustrated by the

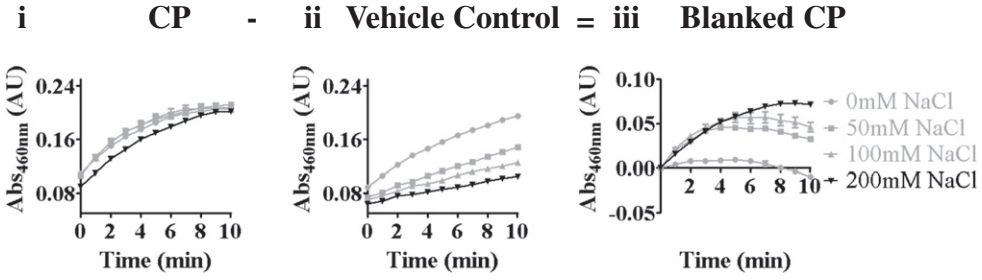

Fig. 4. Effect of varying salinity in HBS for transferrin loading assay. Salinity in HBS (pH 7.2) on the TF loading assay was investigated between 0 and 200 mM NaCl in the presence of CP (250 nM) (i), the corresponding vehicle control (ii) and with CP blanked against the vehicle control (iii). The results in black indicate the most suitable salinity to be close to 200 mM NaCl with all other assay reagents at previously determined concentrations, at 24 °C. As physiological levels of salinity are ~150 mM, and would provide similar rates of activity for CP as shown for 200 mM NaCl, experiments were conducted twice with individual data points of the graphs representing means ± S.E. ΔAbs_{460} shown is of 1 representative experiment of 3, with data points as the mean of triplicate readings.

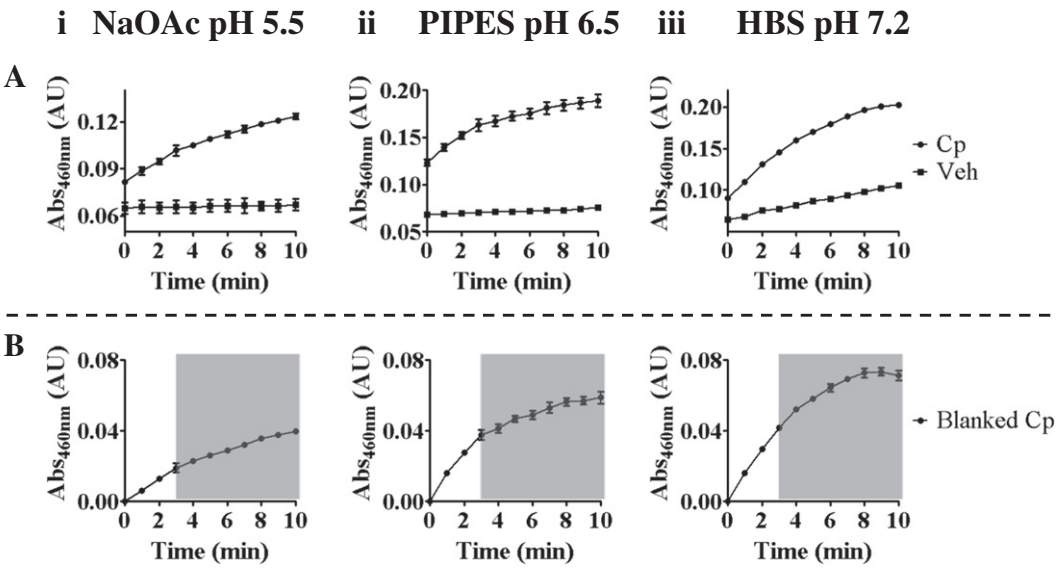

Fig. 5. Recommended conditions selected for the transferrin loading assay. Over a broad pH range the recommended reagent concentrations for the TF loading assay were 50 μM apo-TF 250 nM CP and 100 μM ferrous sulfate. With low pH, the assay had similar conditions to those originally proposed by Johnson et al. [2], but the pH needed to be lowered to 5.5 in order for NaOAc to be within its buffering range (Ai). At higher pH the best conditions were PIPES (Aii) and in the presence of saline, HBS (pH 7.2, 150 mM NaCl) (Aiii). Upon blanking enzymatic activity against vehicle auto-oxidation the recommended time for measuring kinetics at 24 °C in all buffers was within the first 3 min (as shown in black) when enzymatic rate was linear (B). Individual data points of the graphs were means ± S.E. ΔAbs_{460} shown is of 1 representative experiment of 3, with data points as the mean of triplicate readings.

Lineweaver–Burk plots (Fig. 8C & D). Again, similar to above, distortion by competitive auto-oxidation in the TF loading assay means that the inhibition kinetics from the Ferric Gain assay may be more accurate (Fig. 8G, H).

3.6. Minimizing other forms of variability in the ferroxidase assay

Consistency in the preparation of the enzyme studies in the assay was paramount for obtaining reliable kinetics. As an example, CP as provided by the manufacturer was found to contain trace amounts of EDTA that anomalously alter ferroxidase measurements in the assay. Chromatographic exchange of the enzyme buffer to the optimal buffer used in the assay alleviated the inhibitory effect of EDTA previously observed (data not shown).

Similarly, trace contaminants of electrolytes were observed to have varying consequence on ferroxidase activity in the assay. Up to a concentration of 10 mM, sulfate had little effect in the assays, but the

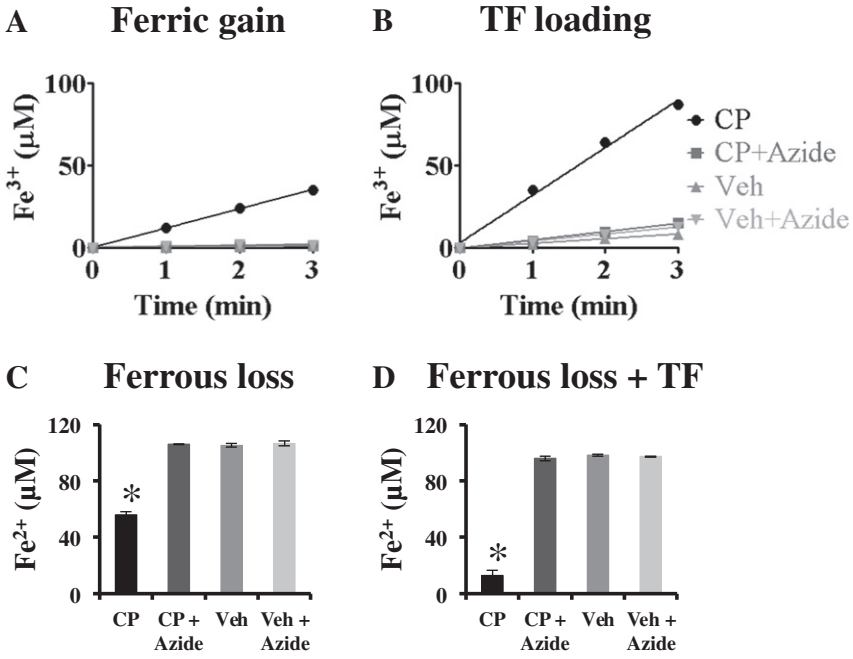

Fig. 6. Ceruloplasmin activity in the triplex ferroxidase assay. Kinetic measurements of CP ferroxidase activity and inhibition with sodium azide were calculated by quantifying (A) the amount of Fe^{3+} produced over 3 min; and (B) the amount of Fe^{3+} loaded onto apo-TF over 3 min. Endpoint measurements of CP ferroxidase activity at 4 min after addition of a Fe^{2+} selective chromogen ferene *S*, which measured the amount of Fe^{2+} remaining after ferroxidase conversion in the absence (C) or presence (D) of transferrin. Final concentrations of the various assay components were: HBS buffer (50 mM HEPES, 150 mM NaCl, pH 7.2); CP (250 nM); sodium azide (1 mM); $FeSO_4$ (100 μM); and apo-TF (50 μM) (only B and D). Temperature was constant at 24 °C throughout the assay. Results in (A) and (B) were blanked against the reading at the first time point. This experiment was performed multiple times. The individual data points shown are means ± S.E., n = 3 of a representative experiment carried out 3 times.

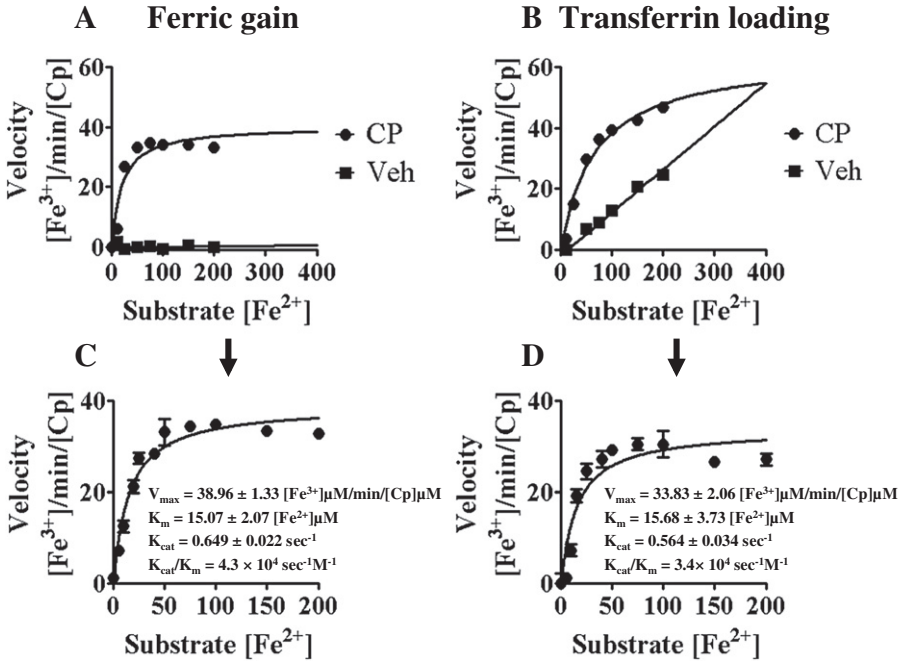

Fig. 7. Characterizing the enzyme kinetics of ceruloplasmin with Ferric Gain and transferrin loading assays run concurrently. Plots representing raw kinetics blanked against 0 μM substrate of both CP activity and vehicle control auto-oxidation for (A) Ferric Gain, and (B) transferrin loading. Michaelis–Menten enzyme kinetics of CP blanked against auto-oxidation was measured by Ferric Gain (C) and TF loading (D). Conditions of the assays were as previously described at varying substrate concentrations ($FeSO_4$ 0–200 μM). The individual data points shown are means ± S.E., n = 3 of a representative experiment, n = 2.

phosphate anion increased the rate of Fe^{2+} oxidation (as measured by Ferric Gain assay) as well as TF loading, and bicarbonates increased TF loading only (Fig. 9). This would explain the increased TF loading in PBS observed in Figs. 2 and S2. Cations Na, K, Ca and Mg up to 10 mM had no effect on the Ferric Gain or TF loading assays (data not shown).

4. Discussion

For nearly 50 years the TF assay has been widely considered by biologists as an ideal method for measuring ferroxidase activity because it emulates a physiological transfer. However, since the assay was published, doubts about its accuracy in measuring kinetic enzyme activity have arisen because it relies on an indirect colorimetric readout of holo-TF, and TF interaction may impact on the enzyme's activity. A further concern has been the use of non-physiological low pH, in order to reduce auto-oxidative interference in this classical assay. Therefore, we investigated whether the assay could be modified to measure enzymatic activity of a ferroxidase under physiological conditions, as well as providing internal controls to ensure authentic ferroxidase kinetics.

4.1. Optimal parameters for measuring ferroxidase activity

Upon evaluating the existing parameters used for the TF loading assay, enzyme, TF, substrate and buffer concentrations were all found to be within an acceptable range to measure ferroxidase activity (Fig. 1). However, the pH 6.0 used for NaOAc buffer was outside its optimal buffering range (3.6–5.6) and thus alternative buffers were identified according to their buffering capabilities at low pH, neutral pH and physiological pH. While NaOAc was still considered the best buffer to use once in its correct buffering range (pH 5.5), Good's buffers PIPES and HEPES were recommended for neutral and physiological pH respectively. With increasing alkalinity ferroxidase activity was augmented, resulting in enhanced sensitivity, however beyond pH 7 the background auto-oxidation rate also increased exponentially and impaired accurate enzymatic rate readings (Fig. 3Di). Increasing salinity in the reaction significantly reduced auto-oxidation rate above pH 7, while minimally affecting ferroxidase activity (Fig. 4). Increasing the salinity of the reaction had the additional benefits of providing a more physiologically relevant environment as well as slowing the enzymatic reaction, which permitted more accurate kinetic readings.

Within the same physiological buffer, additional recommended requisites for measuring enzymatic activity are: (A) an assay temperature of 24 °C instead of 37 °C to slow completion of iron oxidation to >5 min, facilitating kinetic monitoring, (B) elimination of contaminants such as anions or chelators that can affect enzymatic activity (Figs. 2 and 9), (C) auto-injection of substrate and immediate spectrophotometric measuring to minimize discrepancies between reaction start times, and (D) selecting data within the first 3 min of the kinetic assay to ensure that the reaction is within its linear rate (Fig. 5Bi–iii).

Experimentally deriving extinction coefficients using the recommended conditions for assays of Ferric Loss, Ferric Gain and the amount of Fe^{3+} loaded onto TF gave us more precise measurement of iron product concentrations (Table 1). Extinction coefficients at 465 nm for diferric-, C-terminal monoferric- and N-terminal monoferric TFs were previously determined as 4.86, 2.78 and 2.08 mM^{-1} cm^{-1} respectively [53] whereas at 460 nm diferric-TF has previously been calculated as 4.56 mM^{-1} cm^{-1} [39]. In our conditions with PIPES and HBS buffer, the amounts of Fe^{3+} loaded onto TF at 460 nm were 2.28 and 2.02 mM^{-1} cm^{-1} respectively. These values relate well with the extinction coefficients previously reported for monoferric TF [53], without discerning for terminal TF loading, and suggest that the extinction coefficients for Fe^{3+} correspond better with monoferric TF formation rather than diferric TF in physiological conditions and excess TF. Of relevance to the original assay conditions, we were unable to accurately derive an extinction coefficient for the TF loading assay in NaOAc buffer pH 5.5 (0.756 mM^{-1} cm^{-1}; Table 1) despite extinction coefficients for Ferrous Loss and Ferric Gain assays being comparable within all three buffers. This suggests that at low pH, TF is unable to be suitably loaded with Fe^{3+}, resulting in an underestimation of Fe^{3+} production in the previous literature that has used this protocol.

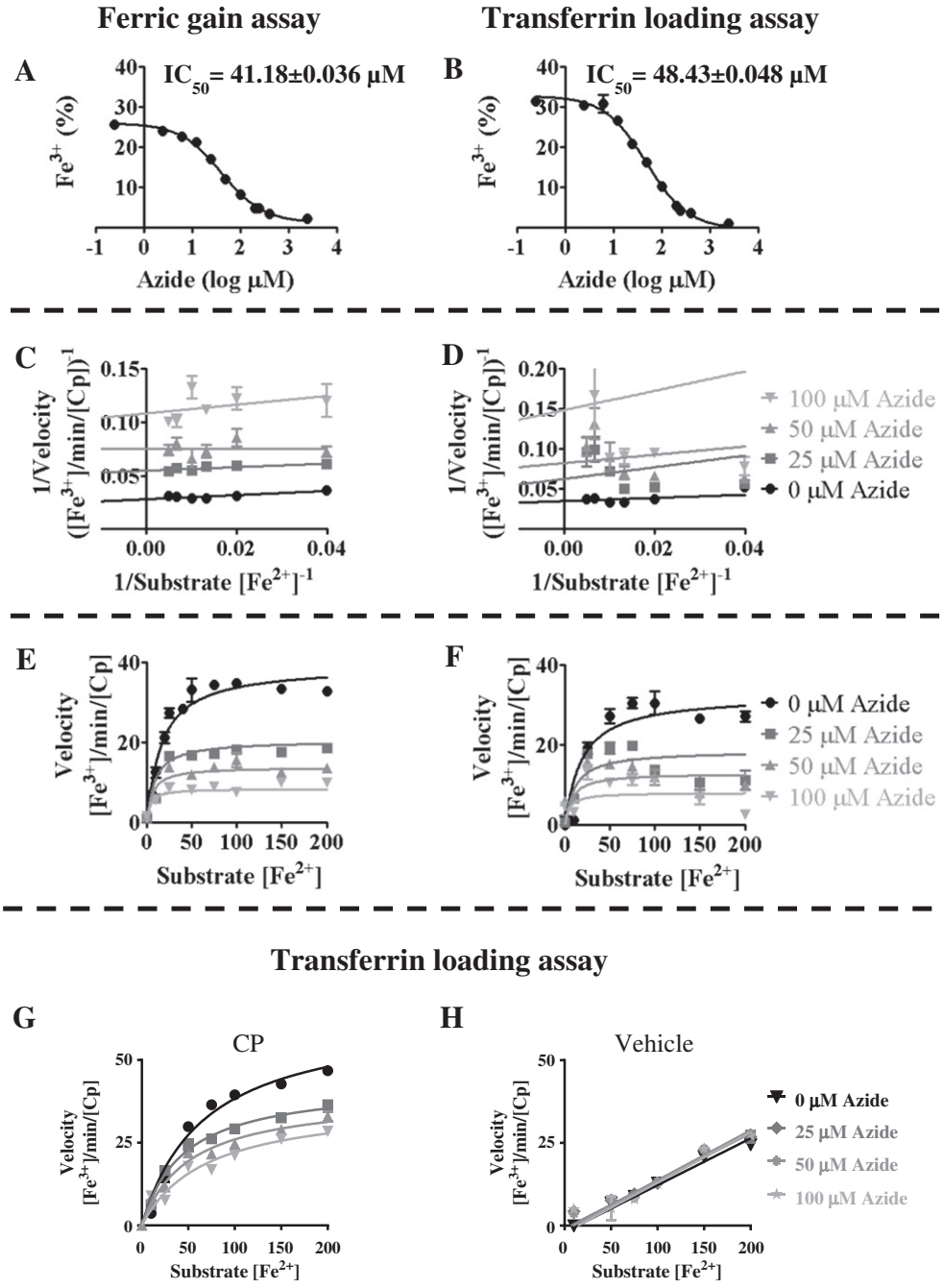

Fig. 8. Characterizing azide inhibition of ceruloplasmin. Sodium azide concentration (0–100 μM) was plotted against the amount of Fe^{3+} converted by CP within 3 min as determined by (A) Ferric Gain or (B) TF loading assays. Lineweaver–Burk (C & D) and a representative nonlinear regression graphical model (E & F) of CP ferroxidase kinetics inhibited by sodium azide were calculated by Ferric Gain and TF loading assays, respectively. Enzymatic kinetics of (G) CP and (H) vehicle alone were determined by transferrin loading assay at 24 °C in the presence of various azide concentrations. Conditions of the assays were as previously described at varying substrate concentrations ($FeSO_4$ 0–200 μM). The individual data points shown are means ± S.E., n = 3 of a representative experiment, n = 2.

4.2. A new triplex assay for measuring ferroxidase activity

This novel three-in-one ferroxidase protocol has the advantage of simultaneously measuring the ability of a ferroxidase to reduce levels of the substrate Fe^{2+}, its conversion to Fe^{3+} and the physiological uptake by apo-TF. The requirement of ferene *S* to measure ferrous loss meant that this part of the assay is only used as the end point control for Fe^{2+} consumption during the ferroxidase reaction. Whereas the Ferric Gain assay directly measures Fe^{3+} conversion over time and therefore can be implemented for the most accurate measurement of enzyme kinetics and inhibition constants involved with a ferroxidase.

The dissociation constant of Fe^{3+} bound to TF is approximately 10^{22} M^{-1} at pH 6.0 [54] and was utilized to indirectly measure iron bound to TF as the product. TF affinity for Fe^{2+} is known to be a lot weaker, but no direct binding data is currently available despite estimates ranging from log *K* 2.5–3.7, depending on the binding sites on TF [55,56]. Whether Fe^{2+} is oxidized before or after uptake into TF (as illustrated in Eqs. (4) and (5)) is yet to be identified and the focus of our future research. Either way, the association of iron with TF could directly affect oxidation rate. Our results on CP kinetics indicate that, at least in the initial substrate concentrations, TF loading proceeded at almost identical K_m as that of Ferric Gain (Fig. 7). This

Table 2
CP enzyme kinetics and azide inhibition constants.

Global	Ferric Gain assay	Transferrin loading assay
V_{max} (μM Fe^{3+}/min/μM CP)	39.3 ± 1.1	32.6 ± 2.3
K_m (μM Fe^{2+})	16.3 ± 1.7	18.4 ± 5.2
αK_i (μM azide)	27.4 ± 1.6	33.2 ± 4.8

suggests that the K_a of TF and iron is much higher than the K_m and thus not rate limiting. TF loading measurements are also affected by increased auto-oxidative rate at pH 7.2 which resulted in decreased velocity with increased substrate concentrations as the rate of auto-oxidation begins to approach the ferroxidation rate. While these complications raise doubts into its use for measuring ferroxidase kinetics, the study of ferroxidase activity as a function of TF loading is especially revealing in regard to the mechanism of diferric TF formation by an enzyme and therefore provides important additional information under physiological conditions.

4.3. Kinetics for ceruloplasmin activity and inhibition by sodium azide within physiological parameters

In vitro enzyme kinetics of purified CP have previously been investigated as a function of oxygen consumption [38], oxidation of *N,N*-dimethyl-*p*-phenylenediamine (DPD) [57] and the non-kinetic formation of diferric TF [33]. As far as we are aware, this is the first time the ferroxidase kinetics of CP has been described under physiological conditions following the direct production of Fe^{3+} and it's loading onto TF. The most direct comparison of CP enzyme kinetics to our assay is by oxygen consumption conducted in acetate buffer at a pH outside acetate's buffering range (pH 7) [38]. Despite this their V_{max} and K_m values are within the general vicinity of our measurements (V_{max} 62.9 μM O_2/min/μM CP and K_m 18.2 μM O_2).

A direct quantification of the inhibitory kinetics of sodium azide on CP ferroxidase activity has also, to our knowledge, not been reported previously, although there are reports of the inhibitory effect of azide on the amine oxidase activity of CP using *p*-phenylenediamine as a substrate [50], and of the inhibitory effect of azide on serum ferroxidase activity (assumed to originate from CP) by TF loading assay [51]. 3 μM azide was reported to inhibit 50% of 380 nM CP amine oxidase activity, however our results demonstrated that azide has 20–25 fold less potency at inhibiting CP ferroxidase activity, consistent with the differences in the reaction mechanisms between the amine oxidase and the ferroxidase activity of CP.

4.4. Implications for measuring ferroxidase activity in a biological environment

Anions such as bicarbonates and phosphates accelerate iron oxidation, as well as promote Fe^{3+} loading into TF. This could be a source of artifact in ferroxidase assays in buffers containing these anions (e.g. PBS) or in biological fluids. As detailed here, controls are required to eliminate the non-enzymatic component when measuring activity in biological samples and may explain the identification of a 'small molecular ferroxidase' within biological samples [20,21].

In synergy with an anion, TF can bind a variety of metal ions such as Fe^{3+}, Al^{3+} and Cu^{2+} with variable affinity. It is proposed that the anion serves as a bridging ligand between the metal and TF [58–60], and in so doing excludes water from two coordination sites [54,61]. In the presence of an anion, ferric-TF is resistant to almost all but the strongest chelators, but without the anion Fe^{3+} binding to TF is negligible. Carbonate is the naturally occurring synergistic anion that forms the strongest metal complexes with TF [58], however, other biologically relevant anions are able to act similarly, depending on their size and the presences of a carboxylate group that brings together TF and Lewis base atoms (i.e. oxygen, nitrogen or sulfur) to interact with the metal [58,61–65].

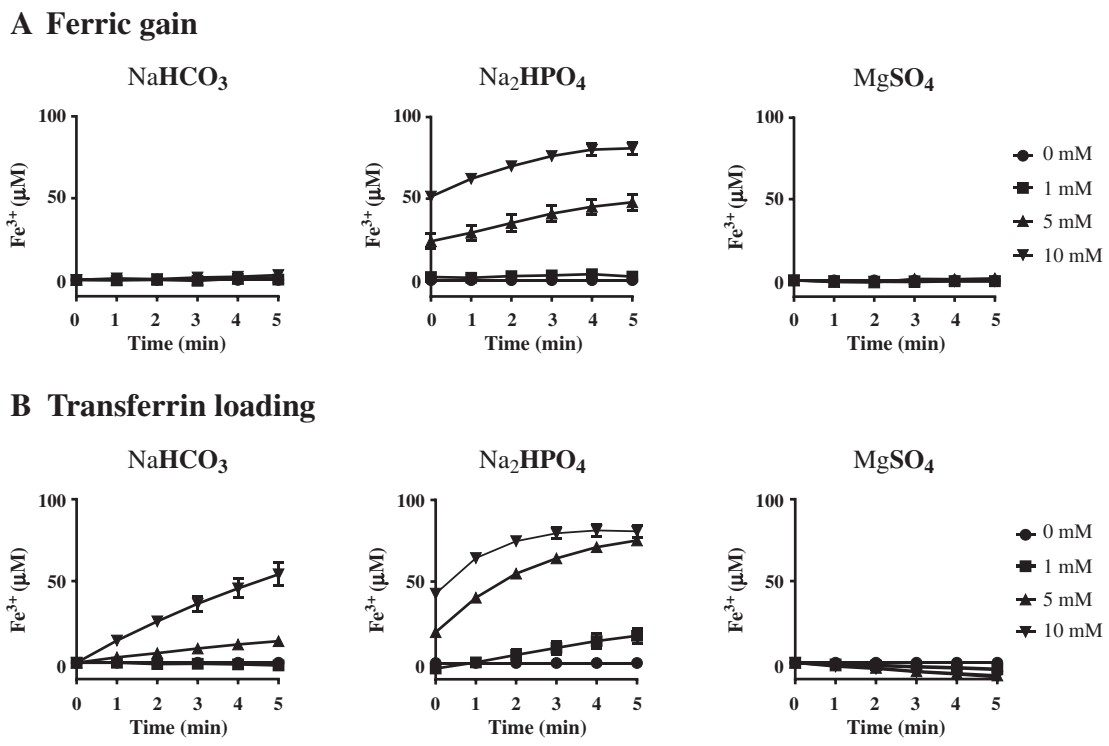

Fig. 9. Effects of various anions on the transferrin loading assay. Bicarbonates, phosphates and sulfates were measured in the (A) Ferric Gain and (B) transferrin loading assays, at 24 °C. Final concentrations of the various assay components were as previously optimized (100 μM $FeSO_4$ and 50 μM apo-TF for (B)) but with 50 mM HBS (pH 7.2) containing variable anions (1, 5 and 10 mM). Individual data points are means ± S.E., n = 3, representative of 2 experiments.

It is widely considered that a ferroxidase facilitates the efflux of cellular iron. In the presence of CP, it has been demonstrated that the enzyme not only stabilizes the iron efflux pore, FPN, on the cell surface but also facilitates the release of Fe^{2+} within the pore through the safe oxidation to Fe^{3+} and its incorporation into apo-TF present in the interstitial fluid surrounding the cell. However, in light of our current findings, and considering existing knowledge described above, it is possible that if a protein is able to stabilize FPN on the cell surface then ferroxidase activity from the same protein may not always be necessary for iron efflux. In a normal physiological environment, levels of bicarbonates and phosphates surrounding the cell are high enough to enable the oxidation of iron at the exit of the FPN pore, as well as to load holo-TF. The observation that a higher anion gap and lower bicarbonate level are associated with higher ferritin levels in a study of 4525 healthy adults [66] supports this possibility. While this non-enzymatic reaction is likely to produce hydroxyl radicals, anti-oxidant buffering in place within the extracellular environment would be more than capable of negating their potential to cause oxidative damage. However, in situations of high oxidative stress or where high rates of cellular iron efflux are required, a ferroxidase such as CP may be essential to safely remove intracellular iron. Our data support the proposition by Kosman [19] that dual routes of cellular iron efflux may exist: a ferroxidase route for expedited removal of iron from FPN with incorporation into TF, and a passive, non-enzymatic route that only requires a membrane bound protein to stabilize FPN on the surface but capitalizes on the oxidative capability of anions within the extracellular environment to facilitate iron release from FPN and incorporation into TF. Further research is currently underway to investigate the biological viability of this second iron efflux model and the pathological relevance of its impairment in disease.

Acknowledgements

Work carried out in Australia was supported by funding from the National Health & Medical Research Council (NHMRC) (#1025774), and work based in the UK was funded by Alzheimer's Research UK (#ART-SRF2011-1) and European Research Council (#334454). The Florey Institute of Neuroscience and Mental Health acknowledges support from the Victorian Government and in particular the funding from the Operational Infrastructure Support Grant.

Appendix A. Supplementary data

Supplementary data to this article can be found online at http://dx.doi.org/10.1016/j.bbagen.2014.08.006.

References

[1] K.J. Waldron, J.C. Rutherford, D. Ford, N.J. Robinson, Metalloproteins and metal sensing, Nature 460 (2009) 823–830.
[2] D.A. Johnson, S. Osaki, E. Frieden, A micromethod for the determination of ferroxidase (ceruloplasmin) in human serums, Clin. Chem. 13 (1967) 142–150.
[3] F. Haber, J. Weiss, The catalytic decomposition of hydrogen peroxide by iron salts, Proc. R. Soc. Lond. A Math. Phys. Sci. 147 (1934) 332–351.
[4] H.J.H. Fenton, LXXIII.—Oxidation of tartaric acid in presence of iron, J. Chem. Soc. Trans. 65 (1894) 899–910.
[5] K.J. Davies, Protein damage and degradation by oxygen radicals. I. General aspects, J. Biol. Chem. 262 (1987) 9895–9901.
[6] T.F. Slater, Free radical mechanisms in tissue injury, in: L.E. Cañedo, L.E. Todd, L. Packer, J. Jaz (Eds.), Cell Function and Disease, Springer, US, 1988, pp. 209–218.
[7] S.P. Wolff, A. Garner, R.T. Dean, Free radicals, lipids and protein degradation, Trends Biochem. Sci. 11 (1986) 27–31.
[8] T.A. Rouault, Iron metabolism in the CNS: implications for neurodegenerative diseases, Nat. Rev. Neurosci. 14 (2013) 551–564.
[9] I. De Domenico, D.M. Ward, M.C. di Patti, S.Y. Jeong, S. David, G. Musci, J. Kaplan, Ferroxidase activity is required for the stability of cell surface ferroportin in cells expressing GPI-ceruloplasmin, EMBO J. 26 (2007) 2823–2831.
[10] O. Han, E.Y. Kim, Colocalization of ferroportin-1 with hephaestin on the basolateral membrane of human intestinal absorptive cells, J. Cell. Biochem. 101 (2007) 1000–1010.
[11] H. Chen, Z.K. Attieh, T. Su, B.A. Syed, H. Gao, R.M. Alaeddine, T.C. Fox, J. Usta, C.E. Naylor, R.W. Evans, A.T. McKie, G.J. Anderson, C.D. Vulpe, Hephaestin is a ferroxidase that maintains partial activity in sex-linked anemia mice, Blood 103 (2004) 3933–3939.
[12] R.C. McCarthy, D.J. Kosman, Ferroportin and exocytoplasmic ferroxidase activity are required for brain microvascular endothelial cell iron efflux, J. Biol. Chem. 288 (2013) 17932–17940.
[13] E. Nemeth, T. Ganz, Regulation of iron metabolism by hepcidin, Annu. Rev. Nutr. 26 (2006) 323–342.
[14] S. Osaki, D.A. Johnson, Mobilization of liver iron by ferroxidase (ceruloplasmin), J. Biol. Chem. 244 (1969) 5757–5758.
[15] H.A. Ragan, S. Nacht, G.R. Lee, C.R. Bishop, G.E. Cartwright, Effect of ceruloplasmin on plasma iron in copper-deficient swine, Am. J. Physiol. 217 (1969) 1320–1323.
[16] H.P. Roeser, G.R. Lee, S. Nacht, G.E. Cartwright, The role of ceruloplasmin in iron metabolism, J. Clin. Invest. 49 (1970) 2408–2417.
[17] X. Xu, S. Pin, M. Gathinji, R. Fuchs, Z.L. Harris, Aceruloplasminemia: an inherited neurodegenerative disease with impairment of iron homeostasis, Ann. N. Y. Acad. Sci. 1012 (2004) 299–305.
[18] L.A. Meyer, A.P. Durley, J.R. Prohaska, Z.L. Harris, Copper transport and metabolism are normal in aceruloplasminemic mice, J. Biol. Chem. 276 (2001) 36857–36861.
[19] D.J. Kosman, Iron metabolism in aerobes: managing ferric iron hydrolysis and ferrous iron autoxidation, Coord. Chem. Rev. 257 (2013) 210–217.
[20] L.W. Gray, T.Z. Kidane, A. Nguyen, S. Akagi, K. Petrasek, Y.L. Chu, A. Cabrera, K. Kantardjieff, A.Z. Mason, M.C. Linder, Copper proteins and ferroxidases in human plasma and that of wild-type and ceruloplasmin knockout mice, Biochem. J. 419 (2009) 237–245.
[21] S. Haldar, J. Beveridge, J. Wong, A. Singh, D. Galimberti, B. Borroni, X. Zhu, J. Blevins, J. Greenlee, G. Perry, C.K. Mukhopadhyay, C. Schmotzer, N. Singh, A low-molecular-weight ferroxidase is increased in the CSF of sCJD cases: CSF ferroxidase and transferrin as diagnostic biomarkers for sCJD, Antioxid. Redox Signal. 19 (2013) 1662–1675.
[22] K.J. Bharucha, J.K. Friedman, A.S. Vincent, E.D. Ross, Lower serum ceruloplasmin levels correlate with younger age of onset in Parkinson's disease, J. Neurol. 255 (2008) 1957–1962.
[23] L. Jin, J. Wang, H. Jin, G. Fei, Y. Zhang, W. Chen, L. Zhao, N. Zhao, X. Sun, M. Zeng, C. Zhong, Nigral iron deposition occurs across motor phenotypes of Parkinson's disease, Eur. J. Neurol. 19 (2012) 969–976.
[24] L. Jin, J. Wang, L. Zhao, H. Jin, G. Fei, Y. Zhang, M. Zeng, C. Zhong, Decreased serum ceruloplasmin levels characteristically aggravate nigral iron deposition in Parkinson's disease, Brain 134 (2011) 50–58.
[25] R. Martinez-Hernandez, S. Montes, J. Higuera-Calleja, P. Yescas, M.C. Boll, A. Diaz-Ruiz, C. Rios, Plasma ceruloplasmin ferroxidase activity correlates with the nigral sonographic area in Parkinson's disease patients: a pilot study, Neurochem. Res. 36 (2011) 2111–2115.
[26] G. Torsdottir, J. Kristinsson, J. Snaedal, T. Johannesson, Ceruloplasmin and iron proteins in the serum of patients with Alzheimer's disease, Dement. Geriatr. Cogn. Disord. Extra 1 (2011) 366–371.
[27] G. Torsdottir, J. Kristinsson, S. Sveinbjornsdottir, J. Snaedal, T. Johannesson, Copper, ceruloplasmin, superoxide dismutase and iron parameters in Parkinson's disease, Pharmacol. Toxicol. 85 (1999) 239–243.
[28] M.C. Boll, M. Alcaraz-Zubeldia, S. Montes, C. Rios, Free copper, ferroxidase and SOD1 activities, lipid peroxidation and NO(x) content in the CSF. A different marker profile in four neurodegenerative diseases, Neurochem. Res. 33 (2008) 1717–1723.
[29] M.C. Boll, J. Sotelo, E. Otero, M. Alcaraz-Zubeldia, C. Rios, Reduced ferroxidase activity in the cerebrospinal fluid from patients with Parkinson's disease, Neurosci. Lett. 265 (1999) 155–158.
[30] S. Olivieri, A. Conti, S. Iannaccone, C.V. Cannistraci, A. Campanella, M. Barbariga, F. Codazzi, I. Pelizzoni, G. Magnani, M. Pesca, D. Franciotta, S.F. Cappa, M. Alessio, Ceruloplasmin oxidation, a feature of Parkinson's disease CSF, inhibits ferroxidase activity and promotes cellular iron retention, J. Neurosci. 31 (2011) 18568–18577.
[31] S. Ayton, P. Lei, J.A. Duce, B.X. Wong, A. Sedjahtera, P.A. Adlard, A.I. Bush, D.I. Finkelstein, Ceruloplasmin dysfunction and therapeutic potential for Parkinson disease, Ann. Neurol. 73 (2013) 554–559.
[32] R. Squitti, C. Salustri, M. Siotto, M. Ventriglia, F. Vernieri, D. Lupoi, E. Cassetta, P.M. Rossini, Ceruloplasmin/transferrin ratio changes in Alzheimer's disease, Int. J. Alzheimers Dis. 2011 (2010) 231595.
[33] J.A. Duce, A. Tsatsanis, M.A. Cater, S.A. James, E. Robb, K. Wikhe, S.L. Leong, K. Perez, T. Johanssen, M.A. Greenough, H.H. Cho, D. Galatis, R.D. Moir, C.L. Masters, C. McLean, R.E. Tanzi, R. Cappai, K.J. Barnham, G.D. Ciccotosto, J.T. Rogers, A.I. Bush, Iron-export ferroxidase activity of beta-amyloid precursor protein is inhibited by zinc in Alzheimer's disease, Cell 142 (2010) 857–867.
[34] G. Bartzokis, J.L. Cummings, C.H. Markham, P.Z. Marmarelis, L.J. Treciokas, T.A. Tishler, S.R. Marder, J. Mintz, MRI evaluation of brain iron in earlier- and later-onset Parkinson's disease and normal subjects, Magn. Reson. Imaging 17 (1999) 213–222.
[35] G. Bartzokis, D. Sultzer, J. Cummings, L.E. Holt, D.B. Hance, V.W. Henderson, J. Mintz, In vivo evaluation of brain iron in Alzheimer disease using magnetic resonance imaging, Arch. Gen. Psychiatry 57 (2000) 47–53.
[36] G. Bartzokis, T.A. Tishler, I.S. Shin, P.H. Lu, J.L. Cummings, Brain ferritin iron as a risk factor for age at onset in neurodegenerative diseases, Ann. N. Y. Acad. Sci. 1012 (2004) 224–236.
[37] E.P. Raven, P.H. Lu, T.A. Tishler, P. Heydari, G. Bartzokis, Increased iron levels and decreased tissue integrity in hippocampus of Alzheimer's disease detected in vivo with magnetic resonance imaging, J. Alzheimers Dis. 37 (2013) 127–136.
[38] S. Osaki, D.A. Johnson, E. Frieden, The possible significance of the ferrous oxidase activity of ceruloplasmin in normal human serum, J. Biol. Chem. 241 (1966) 2746–2751.

[39] G.R. Bakker, R.F. Boyer, Iron incorporation into apoferritin. The role of apoferritin as a ferroxidase, J. Biol. Chem. 261 (1986) 13182–13185.
[40] T.A. Griffiths, A.G. Mauk, R.T. MacGillivray, Recombinant expression and functional characterization of human hephaestin: a multicopper oxidase with ferroxidase activity, Biochemistry 44 (2005) 14725–14731.
[41] D. de Silva, S. Davis-Kaplan, J. Fergestad, J. Kaplan, Purification and characterization of Fet3 protein, a yeast homologue of ceruloplasmin, J. Biol. Chem. 272 (1997) 14208–14213.
[42] O. Erel, Automated measurement of serum ferroxidase activity, Clin. Chem. 44 (1998) 2313–2319.
[43] E. Graf, J.R. Mahoney, R.G. Bryant, J.W. Eaton, Iron-catalyzed hydroxyl radical formation. Stringent requirement for free iron coordination site, J. Biol. Chem. 259 (1984) 3620–3624.
[44] G. Minotti, M. Ikeda-Saito, Fe(II) oxidation and Fe(III) incorporation by the M(r) 66,000 microsomal iron protein that stimulates NADPH oxidation, J. Biol. Chem. 267 (1992) 7611–7614.
[45] D.C. Harris, P. Aisen, Facilitation of Fe(II) autoxidation by Fe(3) complexing agents, Biochim. Biophys. Acta 329 (1973) 156–158.
[46] R.M.C. Dawson, Data for Biochemical Research, 3rd ed. Clarendon Press, Oxford, 1986.
[47] X. Yang, N.D. Chasteen, Ferroxidase activity of ferritin: effects of pH, buffer and Fe(II) and Fe(III) concentrations on Fe(II) autoxidation and ferroxidation, Biochem. J. 338 (Pt 3) (1999) 615–618.
[48] K.D. Welch, T.Z. Davis, S.D. Aust, Iron autoxidation and free radical generation: effects of buffers, ligands, and chelators, Arch. Biochem. Biophys. 397 (2002) 360–369.
[49] K.H. Ebrahimi, P.L. Hagedoorn, W.R. Hagen, A synthetic peptide with the putative iron binding motif of amyloid precursor protein (APP) does not catalytically oxidize iron, PLoS One 7 (2012) e40287.
[50] G. Curzon, The inhibition of caeruloplasmin by azide, Biochem. J. 100 (1966) 295–302.
[51] R.W. Topham, E. Frieden, Identification and purification of a non-ceruloplasmin ferroxidase of human serum, J. Biol. Chem. 245 (1970) 6698–6705.
[52] R.A. Copeland, Evaluation of Enzyme Inhibitors in Drug Discovery: A Guide for Medicinal Chemists and Pharmacologists, Wiley-Interscience, Hoboken, N.J., 2005
[53] E. Frieden, P. Aisen, Forms of iron transferrin, Trends Biochem. Sci. 5 (1980) (X).
[54] P. Aisen, I. Listowsky, Iron transport and storage proteins, Annu. Rev. Biochem. 49 (1980) 357–393.
[55] W.R. Harris, Estimation of the ferrous-transferrin binding constants based on thermodynamic studies of nickel(II)-transferrin, J. Inorg. Biochem. 27 (1986) 41–52.
[56] N. Kojima, G.W. Bates, The formation of Fe3+-transferrin-CO3(2−) via the binding and oxidation of Fe2+, J. Biol. Chem. 256 (1981) 12034–12039.
[57] R.A. Løvstad, A comparative study of the two different activities of ceruloplasmin in human sera, Eur. J. Biochem. 8 (1969) 303–306.
[58] P. Aisen, R. Aasa, B.G. Malmstrom, T. Vanngard, Bicarbonate and the binding of iron to transferrin, J. Biol. Chem. 242 (1967) 2484–2490.
[59] V.L. Pecoraro, W.R. Harris, C.J. Carrano, K.N. Raymond, Siderophilin metal coordination. Difference ultraviolet spectroscopy of di-, tri-, and tetravalent metal ions with ethylenebis[(o-hydroxyphenyl)glycine], Biochemistry 20 (1981) 7033–7039.
[60] A.T. Tan, R.C. Woodworth, Ultraviolet difference spectral studies of conalbumin complexes with transition metal ions, Biochemistry 8 (1969) 3711–3716.
[61] M.S. Shongwe, C.A. Smith, E.W. Ainscough, H.M. Baker, A.M. Brodie, E.N. Baker, Anion binding by human lactoferrin: results from crystallographic and physicochemical studies, Biochemistry 31 (1992) 4451–4458.
[62] J. Dubach, B.J. Gaffney, K. More, G.R. Eaton, S.S. Eaton, Effect of the synergistic anion on electron paramagnetic resonance spectra of iron–transferrin anion complexes is consistent with bidentate binding of the anion, Biophys. J. 59 (1991) 1091–1100.
[63] A.A. Foley, G.W. Bates, The influence of inorganic anions on the formation and stability of Fe3+–transferrin–anion complexes, Biochim. Biophys. Acta 965 (1988) 154–162.
[64] T.B. Rogers, R.E. Feeney, C.F. Meares, Interaction of anions with iron–transferrin–chelate complexes, J. Biol. Chem. 252 (1977) 8108–8112.
[65] M.R. Schlabach, G.W. Bates, The synergistic binding of anions and Fe3+ by transferrin. Implications for the interlocking sites hypothesis, J. Biol. Chem. 250 (1975) 2182–2188.
[66] W.R. Farwell, E.N. Taylor, Serum anion gap, bicarbonate and biomarkers of inflammation in healthy individuals in a national survey, CMAJ 182 (2010) 137–141.